Electronic Supplementary Material (ESI) for Inorganic Chemistry Frontiers.

Biological activity of bis(pyrazolylpyridine) and terpiridine Os(II) complexes in presence of biocompatible ionic liquids

Angelina Z. Petrović,[a] Dušan C. Ćoćić,[a] Dirk Bockfeld,[b] Marko Živanović,[c] Nevena Milivojević,[c] Katarina Virijević,[c] Nenad Janković,[c] Andreas Scheurer,[d] Milan Vraneš,[e] Jovana V. Bogojeski[a]*

[a] University of Kragujevac, Faculty of Science, Radoja Domanovića 12, 34000 Kragujevac, Serbia

[b] Institut für Anorganische und Analytische Chemie, Technische Universität Braunschweig, Hagenring 30, 38106 Brauschweig, Germany

[c] University of Kragujevac, Institute for Information Technologies Kragujevac, Department of Science, Jovana Cvijića bb, 34000 Kragujevac, Serbia

[d] Inorganic Chemistry, Department of Chemistry and Pharmacy, University of Erlangen-Nürnberg, 91058 Erlangen, Germany

[e] Department of Chemistry, Biochemistry and Environmental Protection University of Novi Sad, Faculty of Science, Trg Dositeja Obradovića 3, 21000 Novi Sad

**Corresponding author:*

Dr. Jovana Bogojeski

Department of Chemistry

Faculty of Science

University of Kragujevac

Radoja Domanovića 12

Tel: +381(0)34336223

Fax: +381 (0)34 335040

e-mail: jovana.bogojeski@pmf.kg.ac.rs

Table S1. Crystal data and structure refinement of $[Os^{II}(H_2L^{tBut})Cl_2(dmso)]\cdot H_2O\cdot DMSO$.

CCDC	2045190	
Empirical formula	$C_{23}H_{39}Cl_2N_5O_3OsS_2$	
Formula weight	758.81	
Temperature	100(2) K	
Wavelength	1.54184 Å	
Instrument (scan mode)	XtaLAB Synergy, Single source HyPix (ω scan)	
Crystal system	Orthorhombic	
Space group	*Pbca*	
Unit cell dimensions	a = 10.0149(3) Å b = 19.5277(5) Å c = 29.9561(9) Å	α= 90° β= 90° γ = 90°
Volume	5858.5(3) $Å^3$	
Z	8	
Density (calculated)	1.721 Mg/m^3	
Absorption coefficient	11.510 mm^{-1}	
F(000)	3024	
Crystal habitus	needle (black)	
Crystal size	0.078 x 0.020 x 0.012 mm^3	
Theta range for data collection	4.529 to 77.572°	
Index ranges	-12<=h<=12, -24<=k<=23, -31<=l<=37	
Reflections collected	66071	
Independent reflections	6158 [R(int) = 0.0778]	
Completeness to theta = 67.684°	99.9 %	
Absorption correction	Gaussian	
Max. and min. transmission	0.962 and 0.529	
Refinement method	Full-matrix least-squares on F^2	
Data / restraints / parameters	6158 / 0 / 338	
Goodness-of-fit on F^2	1.041	
Final R indices [I>2σ(I)]	R1 = 0.0348, wR2 = 0.0882	
R indices (all data)	R1 = 0.0432, wR2 = 0.0925	
Largest diff. peak and hole	1.458 and -1.462 $e.Å^{-3}$	
Crystallisation Details:	from DMSO/water, r.t.	

Table S2. Atomic coordinates (x 10^4) and equivalent isotropic displacement parameters ($Å^2$x 10^3). U(eq) is defined as one third of the trace of the orthogonalized U_{ij} tensor.

	x	y	z	U(eq)
Os(1)	5575.7(2)	3487.9(2)	6423.0(2)	17.1(1)
Cl(1)	3847.7(10)	4309.5(5)	6491.2(3)	23.6(2)
Cl(2)	7146.3(10)	2593.6(5)	6359.0(3)	22.8(2)
S(1)	5945.1(11)	3799.2(6)	5701.8(3)	23.6(2)
O(1)	5150(4)	3503.1(19)	5333.6(12)	38.6(9)
N(1)	3269(4)	2408.0(18)	6142.3(12)	21.4(7)
N(2)	4064(4)	2739.5(18)	6428.6(11)	19.1(7)
N(3)	5332(3)	3288.5(17)	7083.2(11)	16.6(7)
N(4)	6915(3)	4129.7(17)	6686.7(11)	18.9(7)
N(5)	7704(3)	4632.0(17)	6526.3(12)	19.7(7)
C(1)	1332(5)	1601(2)	6102.1(15)	25.5(9)
C(2)	609(5)	2068(3)	5773.1(18)	35.6(11)
C(3)	2057(5)	1016(3)	5851.5(18)	35.7(11)
C(4)	331(5)	1294(3)	6431.3(17)	31.9(11)
C(5)	2354(4)	2019(2)	6355.5(14)	20.7(8)
C(6)	2584(4)	2101(2)	6808.4(14)	21.1(8)
C(7)	3653(4)	2551(2)	6844.0(13)	18.4(8)
C(8)	4359(4)	2856(2)	7219.6(14)	19.1(8)
C(9)	4124(4)	2762(2)	7669.9(14)	20.5(8)
C(10)	4911(4)	3113(2)	7975.7(14)	20.2(8)
C(11)	5926(4)	3552(2)	7829.3(15)	20.9(8)
C(12)	6106(4)	3641.9(19)	7373.9(13)	17.1(8)
C(13)	6995(4)	4117(2)	7149.4(13)	17.3(8)
C(14)	7894(4)	4610(2)	7278.0(14)	20.2(8)
C(15)	8288(4)	4926(2)	6876.8(14)	21.2(8)
C(16)	9202(4)	5543(2)	6827.9(15)	22.6(9)
C(17)	8661(6)	6109(2)	7133.9(17)	36.8(12)
C(18)	10612(5)	5357(3)	6965(2)	46.7(15)
C(19)	9194(5)	5806(3)	6348.8(17)	32.5(11)
C(20)	5815(5)	4701(3)	5638.8(17)	32.3(11)
C(21)	7658(5)	3706(3)	5553.8(17)	35.4(11)
S(2)	6290.4(13)	732.0(7)	5097.8(5)	39.2(3)
O(2)	4879(4)	936(2)	5184.9(13)	43.0(9)
C(22)	7278(7)	1467(3)	5223(2)	51.0(15)
C(23)	6478(7)	735(4)	4506(2)	62.6(19)
O(3)	3924(4)	2270.9(19)	5266.1(12)	34.4(8)

Table S3. Bond lengths [Å] and angles [°].

Os(1)-N(4)	1.998(3)	C(9)-H(9)	0.9500
Os(1)-N(3)	2.031(3)	C(10)-C(11)	1.400(6)
Os(1)-N(2)	2.104(4)	C(10)-H(10)	0.9500
Os(1)-S(1)	2.2743(10)	C(11)-C(12)	1.387(6)
Os(1)-Cl(2)	2.3581(10)	C(11)-H(11)	0.9500
Os(1)-Cl(1)	2.3687(10)	C(12)-C(13)	1.451(6)
S(1)-O(1)	1.478(4)	C(13)-C(14)	1.374(6)
S(1)-C(20)	1.776(5)	C(14)-C(15)	1.407(6)
S(1)-C(21)	1.781(5)	C(14)-H(14)	0.9500
N(1)-N(2)	1.337(5)	C(15)-C(16)	1.520(6)
N(1)-C(5)	1.351(6)	C(16)-C(18)	1.516(6)
N(1)-H(1)	0.8800	C(16)-C(19)	1.524(7)
N(2)-C(7)	1.361(5)	C(16)-C(17)	1.533(6)
N(3)-C(8)	1.352(5)	C(17)-H(17A)	0.9800
N(3)-C(12)	1.355(5)	C(17)-H(17B)	0.9800
N(4)-N(5)	1.348(5)	C(17)-H(17C)	0.9800
N(4)-C(13)	1.389(5)	C(18)-H(18A)	0.9800
N(5)-C(15)	1.332(5)	C(18)-H(18B)	0.9800
N(5)-H(5)	0.8800	C(18)-H(18C)	0.9800
C(1)-C(5)	1.514(6)	C(19)-H(19A)	0.9800
C(1)-C(2)	1.526(7)	C(19)-H(19B)	0.9800
C(1)-C(4)	1.528(7)	C(19)-H(19C)	0.9800
C(1)-C(3)	1.548(6)	C(20)-H(20A)	0.9800
C(2)-H(2A)	0.9800	C(20)-H(20B)	0.9800
C(2)-H(2B)	0.9800	C(20)-H(20C)	0.9800
C(2)-H(2C)	0.9800	C(21)-H(21A)	0.9800
C(3)-H(3A)	0.9800	C(21)-H(21B)	0.9800
C(3)-H(3B)	0.9800	C(21)-H(21C)	0.9800
C(3)-H(3C)	0.9800	S(2)-O(2)	1.492(4)
C(4)-H(4A)	0.9800	S(2)-C(23)	1.782(7)
C(4)-H(4B)	0.9800	S(2)-C(22)	1.784(6)
C(4)-H(4C)	0.9800	C(22)-H(22A)	0.9800
C(5)-C(6)	1.386(6)	C(22)-H(22B)	0.9800
C(6)-C(7)	1.390(6)	C(22)-H(22C)	0.9800
C(6)-H(6)	0.9500	C(23)-H(23A)	0.9800
C(7)-C(8)	1.457(6)	C(23)-H(23B)	0.9800
C(8)-C(9)	1.382(6)	C(23)-H(23C)	0.9800
C(9)-C(10)	1.389(6)	O(3)-H(3D)	0.8509

O(3)-H(3E)	0.8497	C(5)-C(1)-C(4)	109.3(4)
		C(2)-C(1)-C(4)	109.9(4)
N(4)-Os(1)-N(3)	79.39(14)	C(5)-C(1)-C(3)	108.9(4)
N(4)-Os(1)-N(2)	156.24(13)	C(2)-C(1)-C(3)	110.5(4)
N(3)-Os(1)-N(2)	76.85(13)	C(4)-C(1)-C(3)	109.4(4)
N(4)-Os(1)-S(1)	95.67(10)	C(1)-C(2)-H(2A)	109.5
N(3)-Os(1)-S(1)	174.85(10)	C(1)-C(2)-H(2B)	109.5
N(2)-Os(1)-S(1)	108.07(9)	H(2A)-C(2)-H(2B)	109.5
N(4)-Os(1)-Cl(2)	92.80(10)	C(1)-C(2)-H(2C)	109.5
N(3)-Os(1)-Cl(2)	91.00(10)	H(2A)-C(2)-H(2C)	109.5
N(2)-Os(1)-Cl(2)	88.07(10)	H(2B)-C(2)-H(2C)	109.5
S(1)-Os(1)-Cl(2)	90.70(4)	C(1)-C(3)-H(3A)	109.5
N(4)-Os(1)-Cl(1)	91.80(10)	C(1)-C(3)-H(3B)	109.5
N(3)-Os(1)-Cl(1)	87.58(10)	H(3A)-C(3)-H(3B)	109.5
N(2)-Os(1)-Cl(1)	86.79(10)	C(1)-C(3)-H(3C)	109.5
S(1)-Os(1)-Cl(1)	91.13(4)	H(3A)-C(3)-H(3C)	109.5
Cl(2)-Os(1)-Cl(1)	174.85(4)	H(3B)-C(3)-H(3C)	109.5
O(1)-S(1)-C(20)	105.6(2)	C(1)-C(4)-H(4A)	109.5
O(1)-S(1)-C(21)	107.0(2)	C(1)-C(4)-H(4B)	109.5
C(20)-S(1)-C(21)	98.4(3)	H(4A)-C(4)-H(4B)	109.5
O(1)-S(1)-Os(1)	121.11(15)	C(1)-C(4)-H(4C)	109.5
C(20)-S(1)-Os(1)	110.74(17)	H(4A)-C(4)-H(4C)	109.5
C(21)-S(1)-Os(1)	111.45(18)	H(4B)-C(4)-H(4C)	109.5
N(2)-N(1)-C(5)	111.9(3)	N(1)-C(5)-C(6)	106.6(4)
N(2)-N(1)-H(1)	124.1	N(1)-C(5)-C(1)	121.7(4)
C(5)-N(1)-H(1)	124.1	C(6)-C(5)-C(1)	131.7(4)
N(1)-N(2)-C(7)	106.0(3)	C(5)-C(6)-C(7)	106.0(4)
N(1)-N(2)-Os(1)	139.4(3)	C(5)-C(6)-H(6)	127.0
C(7)-N(2)-Os(1)	114.4(3)	C(7)-C(6)-H(6)	127.0
C(8)-N(3)-C(12)	122.4(4)	N(2)-C(7)-C(6)	109.5(4)
C(8)-N(3)-Os(1)	120.0(3)	N(2)-C(7)-C(8)	116.7(3)
C(12)-N(3)-Os(1)	117.4(3)	C(6)-C(7)-C(8)	133.8(4)
N(5)-N(4)-C(13)	109.6(3)	N(3)-C(8)-C(9)	120.1(4)
N(5)-N(4)-Os(1)	135.1(3)	N(3)-C(8)-C(7)	111.8(4)
C(13)-N(4)-Os(1)	114.9(3)	C(9)-C(8)-C(7)	128.1(4)
C(15)-N(5)-N(4)	106.9(3)	C(8)-C(9)-C(10)	118.8(4)
C(15)-N(5)-H(5)	126.6	C(8)-C(9)-H(9)	120.6
N(4)-N(5)-H(5)	126.6	C(10)-C(9)-H(9)	120.6
C(5)-C(1)-C(2)	108.8(4)	C(9)-C(10)-C(11)	120.5(4)

C(9)-C(10)-H(10)	119.8	C(16)-C(19)-H(19A)	109.5
C(11)-C(10)-H(10)	119.8	C(16)-C(19)-H(19B)	109.5
C(12)-C(11)-C(10)	118.7(4)	H(19A)-C(19)-H(19B)	109.5
C(12)-C(11)-H(11)	120.7	C(16)-C(19)-H(19C)	109.5
C(10)-C(11)-H(11)	120.7	H(19A)-C(19)-H(19C)	109.5
N(3)-C(12)-C(11)	119.6(4)	H(19B)-C(19)-H(19C)	109.5
N(3)-C(12)-C(13)	112.2(3)	S(1)-C(20)-H(20A)	109.5
C(11)-C(12)-C(13)	128.1(4)	S(1)-C(20)-H(20B)	109.5
C(14)-C(13)-N(4)	107.7(3)	H(20A)-C(20)-H(20B)	109.5
C(14)-C(13)-C(12)	136.1(4)	S(1)-C(20)-H(20C)	109.5
N(4)-C(13)-C(12)	116.1(3)	H(20A)-C(20)-H(20C)	109.5
C(13)-C(14)-C(15)	104.6(4)	H(20B)-C(20)-H(20C)	109.5
C(13)-C(14)-H(14)	127.7	S(1)-C(21)-H(21A)	109.5
C(15)-C(14)-H(14)	127.7	S(1)-C(21)-H(21B)	109.5
N(5)-C(15)-C(14)	111.2(4)	H(21A)-C(21)-H(21B)	109.5
N(5)-C(15)-C(16)	122.0(4)	S(1)-C(21)-H(21C)	109.5
C(14)-C(15)-C(16)	126.8(4)	H(21A)-C(21)-H(21C)	109.5
C(18)-C(16)-C(15)	110.1(4)	H(21B)-C(21)-H(21C)	109.5
C(18)-C(16)-C(19)	109.9(4)	O(2)-S(2)-C(23)	105.9(3)
C(15)-C(16)-C(19)	110.8(4)	O(2)-S(2)-C(22)	105.9(3)
C(18)-C(16)-C(17)	109.8(4)	C(23)-S(2)-C(22)	98.5(3)
C(15)-C(16)-C(17)	107.5(4)	S(2)-C(22)-H(22A)	109.5
C(19)-C(16)-C(17)	108.6(4)	S(2)-C(22)-H(22B)	109.5
C(16)-C(17)-H(17A)	109.5	H(22A)-C(22)-H(22B)	109.5
C(16)-C(17)-H(17B)	109.5	S(2)-C(22)-H(22C)	109.5
H(17A)-C(17)-H(17B)	109.5	H(22A)-C(22)-H(22C)	109.5
C(16)-C(17)-H(17C)	109.5	H(22B)-C(22)-H(22C)	109.5
H(17A)-C(17)-H(17C)	109.5	S(2)-C(23)-H(23A)	109.5
H(17B)-C(17)-H(17C)	109.5	S(2)-C(23)-H(23B)	109.5
C(16)-C(18)-H(18A)	109.5	H(23A)-C(23)-H(23B)	109.5
C(16)-C(18)-H(18B)	109.5	S(2)-C(23)-H(23C)	109.5
H(18A)-C(18)-H(18B)	109.5	H(23A)-C(23)-H(23C)	109.5
C(16)-C(18)-H(18C)	109.5	H(23B)-C(23)-H(23C)	109.5
H(18A)-C(18)-H(18C)	109.5	H(3D)-O(3)-H(3E)	104.5
H(18B)-C(18)-H(18C)	109.5		

Table S4. Torsion angles [°].

C(5)-N(1)-N(2)-C(7)	0.6(5)	N(5)-N(4)-C(13)-C(14)	-2.1(5)
C(5)-N(1)-N(2)-Os(1)	-173.0(3)	Os(1)-N(4)-C(13)-C(14)	-176.5(3)
C(13)-N(4)-N(5)-C(15)	0.9(4)	N(5)-N(4)-C(13)-C(12)	174.6(3)
Os(1)-N(4)-N(5)-C(15)	173.8(3)	Os(1)-N(4)-C(13)-C(12)	0.2(4)
N(2)-N(1)-C(5)-C(6)	-0.5(5)	N(3)-C(12)-C(13)-C(14)	175.2(5)
N(2)-N(1)-C(5)-C(1)	179.3(4)	C(11)-C(12)-C(13)-C(14)	-0.7(8)
C(2)-C(1)-C(5)-N(1)	-52.6(5)	N(3)-C(12)-C(13)-N(4)	-0.3(5)
C(4)-C(1)-C(5)-N(1)	-172.6(4)	C(11)-C(12)-C(13)-N(4)	-176.1(4)
C(3)-C(1)-C(5)-N(1)	67.9(5)	N(4)-C(13)-C(14)-C(15)	2.3(4)
C(2)-C(1)-C(5)-C(6)	127.2(5)	C(12)-C(13)-C(14)-C(15)	-173.4(5)
C(4)-C(1)-C(5)-C(6)	7.2(7)	N(4)-N(5)-C(15)-C(14)	0.6(5)
C(3)-C(1)-C(5)-C(6)	-112.2(5)	N(4)-N(5)-C(15)-C(16)	-176.7(4)
N(1)-C(5)-C(6)-C(7)	0.2(5)	C(13)-C(14)-C(15)-N(5)	-1.8(5)
C(1)-C(5)-C(6)-C(7)	-179.6(4)	C(13)-C(14)-C(15)-C(16)	175.3(4)
N(1)-N(2)-C(7)-C(6)	-0.4(5)	N(5)-C(15)-C(16)-C(18)	-115.1(5)
Os(1)-N(2)-C(7)-C(6)	175.0(3)	C(14)-C(15)-C(16)-C(18)	68.1(6)
N(1)-N(2)-C(7)-C(8)	-179.0(3)	N(5)-C(15)-C(16)-C(19)	6.7(6)
Os(1)-N(2)-C(7)-C(8)	-3.6(4)	C(14)-C(15)-C(16)-C(19)	-170.1(4)
C(5)-C(6)-C(7)-N(2)	0.1(5)	N(5)-C(15)-C(16)-C(17)	125.2(4)
C(5)-C(6)-C(7)-C(8)	178.4(4)	C(14)-C(15)-C(16)-C(17)	-51.6(6)
C(12)-N(3)-C(8)-C(9)	0.0(6)		
Os(1)-N(3)-C(8)-C(9)	-174.9(3)		
C(12)-N(3)-C(8)-C(7)	178.8(3)		
Os(1)-N(3)-C(8)-C(7)	3.8(4)		
N(2)-C(7)-C(8)-N(3)	0.0(5)		
C(6)-C(7)-C(8)-N(3)	-178.2(4)		
N(2)-C(7)-C(8)-C(9)	178.7(4)		
C(6)-C(7)-C(8)-C(9)	0.5(8)		
N(3)-C(8)-C(9)-C(10)	-0.6(6)		
C(7)-C(8)-C(9)-C(10)	-179.1(4)		
C(8)-C(9)-C(10)-C(11)	-0.3(6)		
C(9)-C(10)-C(11)-C(12)	1.7(6)		
C(8)-N(3)-C(12)-C(11)	1.4(6)		
Os(1)-N(3)-C(12)-C(11)	176.5(3)		
C(8)-N(3)-C(12)-C(13)	-174.8(3)		
Os(1)-N(3)-C(12)-C(13)	0.2(4)		
C(10)-C(11)-C(12)-N(3)	-2.2(6)		
C(10)-C(11)-C(12)-C(13)	173.4(4)		

Table S5. The constant rates of the substitution reactions of the **Os1-3** complexes with L-Met, 5'-GMP, and GSH at pH = 7.2 (25 mM Hepes buffer/50 mM NaCl).

$[Os^{II}(H_2L^{tBut})Cl_2H_2O]$ (Os1)					
	T(K)	10^4k_2 $M^{-1}s^{-1}$	$10^1k_1[Cl^-]$ $M^{-1}s^{-1}$	$\Delta H_2^{\neq}$ kJ mol^{-1}	$\Delta S_2^{\neq}$ $JK^{-1}mol^{-1}$
L-Met	310	0.39 ± 0.02	1.04 ± 0.04	/	/
5'-GMP	288	1.18 ± 0.36	0.57 ± 0.13	12 ± 1	–154 ± 4
	298	2.30 ± 0.24	0.13 ± 0.73		
	310	2.80 ± 0.28	0.65 ± 0.47		
GSH	310	0.18 ± 0.02	0.87 ± 0.05	/	/
$[Os^{II}(Me_2L^{tBut})Cl_2H_2O]$ (Os2)					
	T(K)	10^4k_2 $M^{-1}s^{-1}$	$10^1k_1[Cl^-]$ $M^{-1}s^{-1}$	$\Delta H_2^{\neq}$ kJ mol^{-1}	$\Delta S_2^{\neq}$ $JK^{-1}mol^{-1}$
L-Met	310	0.34 ± 0.02	0.57 ± 0.03	/	/
5'-GMP	288	1.18 ± 0.10	1.68 ± 0.17	28 ± 2	–102 ± 6
	298	2.29 ± 0.25	5.64 ± 0.42		
	310	2.85 ± 0.18	6.31 ± 0.29		
GSH	310	0.20 ± 0.02	0.77 ± 0.04	/	/
$[Os^{II}(terpy)Cl_2H_2O]$ (Os3)					
	T(K)	10^4k_2 $M^{-1}s^{-1}$	$10^1k_1[Cl^-]$ $M^{-1}s^{-1}$	$\Delta H_2^{\neq}$ kJ mol^{-1}	$\Delta S_2^{\neq}$ $JK^{-1}mol^{-1}$
L-Met	310	0.12 ± 0.02	0.24 ± 0.03	/	/
5'-GMP	288	1.13 ± 0.10	1.69 ± 0.16	12 ± 2	–157 ± 7
	298	1.47 ± 0.11	1.97 ± 0.19		
	310	1.76 ± 0.15	2.34 ± 0.25		
GSH	310	0.17 ± 0.01	0.10 ± 0.03	/	/

Table S6. DNA binding constants (K_b) for the examined osmium complexes and structurally similar rhodium complexes.

	CT-DNA	**Ref.**
	$10^4 K_b$ [M^{-1}]	
$[Os^{II}(H_2L^{tBut})Cl_2H_2O]$ (Os1)	1.43 ± 0.1	***This paper***
$[Os^{II}(Me_2L^{tBut})Cl_2H_2O]$ (Os2)	1.30 ± 0.1	***This paper***
$[Os^{II}(terpy)Cl_2H_2O]$ (Os3)	1.42 ± 0.1	***This paper***
$[Rh^{III}(H_2L^{tBu})Cl_3]$	9.7 ± 0.1	59
$[Rh^{III}(terpy)Cl_3]$	7.0 ± 0.1	24

Table S7. Values of Stern-Volmers constants, K_{sv}, for the examined osmium complexes for fluorescence titrations with CT-DNA/EB (concentration CT-DNA/EB 5μM, ratio complex: DNA was 0.5-5) in the presence of different ionic liquids, IL1-8. Complex-ionic liquids ratio was 1:1, all reactions were performed in PBS.

	Os1	**Os2**	**Os3**
	$10^4 K_{SV}$ [M^{-1}]	$10^4 K_{SV}$ [M^{-1}]	$10^4 K_{SV}$ [M^{-1}]
In absence of IL	4.41 ± 0.1	2.85 ± 0.1	2.63 ± 0.1
IL1	3.46 ± 0.1	3.43 ± 0.1	3.24 ± 0.1
IL2	3.71 ± 0.1	3.66 ± 0.1	3.58 ± 0.1
IL3	3.51 ± 0.1	3.08 ± 0.1	3.22 ± 0.1
IL4	3.19 ± 0.1	2.54 ± 0.1	3.11 ± 0.1
IL5	3.15± 0.1	2.58 ± 0.1	2.76 ± 0.1
IL6	2.86 ± 0.1	2.10 ± 0.1	2.61 ± 0.1
IL7	3.37 ± 0.1	3.09 ± 0.1	3.39 ± 0.1
IL8	3.10 ± 0.1	2.34 ± 0.1	3.06 ± 0.1

Table S8. Values of Stern-Volmers constants, K_b, quenching rate constants k_q, number of binding sites, n, and coloration factor, R, for the examined osmium complexes to HAS molecule.

	$10^4 K_b[M^{-1}]$	$10^{13} k_q[M^{-1}]$	n	R
$[Os^{II}(H_2L^{tBut})Cl_2H_2O]$(Os1)	5.98 ± 0.1	9.74 ± 0.1	1.02	0.9921
$[Os^{II}(Me_2L^{tBut})Cl_2H_2O]$ (Os2)	5.17 ± 0.1	8.43 ± 0.1	0.98	0.9901
$[Os^{II}(terpy)Cl_2H_2O]$ (Os3)	4.56 ± 0.1	7.43 ± 0.1	1.03	0.9893

Table S9. FRET results between complexes Os1-3 and HSA.

Complex	J^a [nm^4/Mcm]	E^b	$R_0{}^c$ [Å]	r^d [Å]
Os1	5.01 x 10^9	0.33	4.71	5.32
Os2	2.02 x 10^9	0.27	4.05	4.76
Os3	8.28 x 10^8	0.25	3.49	4.21

[a] Overlap integral

[b] Energy transfer efficiency

[c] Förster's distance at which energy transfer is 50% efficient

[d] D-A distance

Table S10. Top-score values for investigated complex **Os1** with HSA proteins, with most pronounced interacting amino acid residues.

Serum albumin docking						Interaction with amino acids residues[b]	
PDB ID of SA	Binding site	MolDock	Rerank	HBond	Docking	Steric	Hydrogen bond
1AO6 – humane serum albumin	**I**[a]	-123.94	-74.59	0	-121.88	Phe-206, Trp-214, Ala-213	Arg-209
	I[b]	-115.34	-72.65	-0.14	-166.69		
	II[a]	-97.31	-51.13	0	-87.69	Leu-391, Arg-485, Tyr-411, Phe-403, Asn-391, Iln-388,	Tyr-411
	II[b]	-93.57	-50.16	-0.32	-81.17		

[a]Best complex pose according to MolDock, Docking, and Rerank scoring functions.
[b]Best complex pose according to Hbond scoring function.

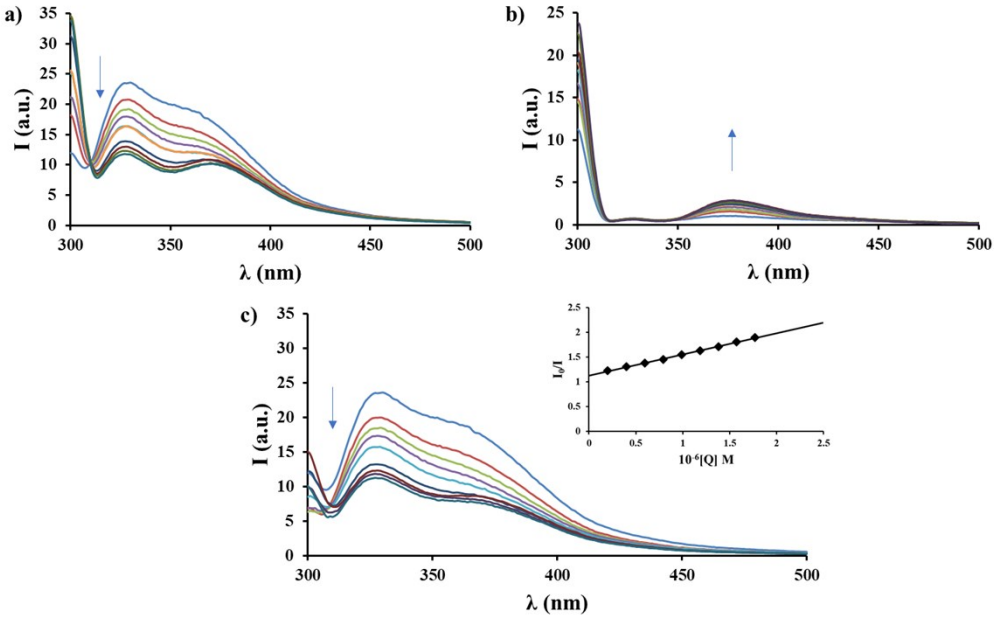

Fig. S1. a) Emission spectra of human serum albumin (2 μM; λex = 295 nm; λem = 365 nm) in the presence of the examined **Os1** complex, ratio complex : serum albumin was 1-10. b) Emission spectra of the examined **Os1** complex in the same concentrations as in spectra recorded with HSA c) Emission spectra of human serum albumin (2 μM; λex = 295 nm; λem = 365 nm) in the presence of the examined **Os1** complex, corrected for the emission spectra of the complex, ratio complex : serum albumin was 1-10. Insert graph: The dependence of I_0/I on the concentration [Q] (Q =

complex). Arrows show changes in intensity after adding solutions of the growing concentration complex.

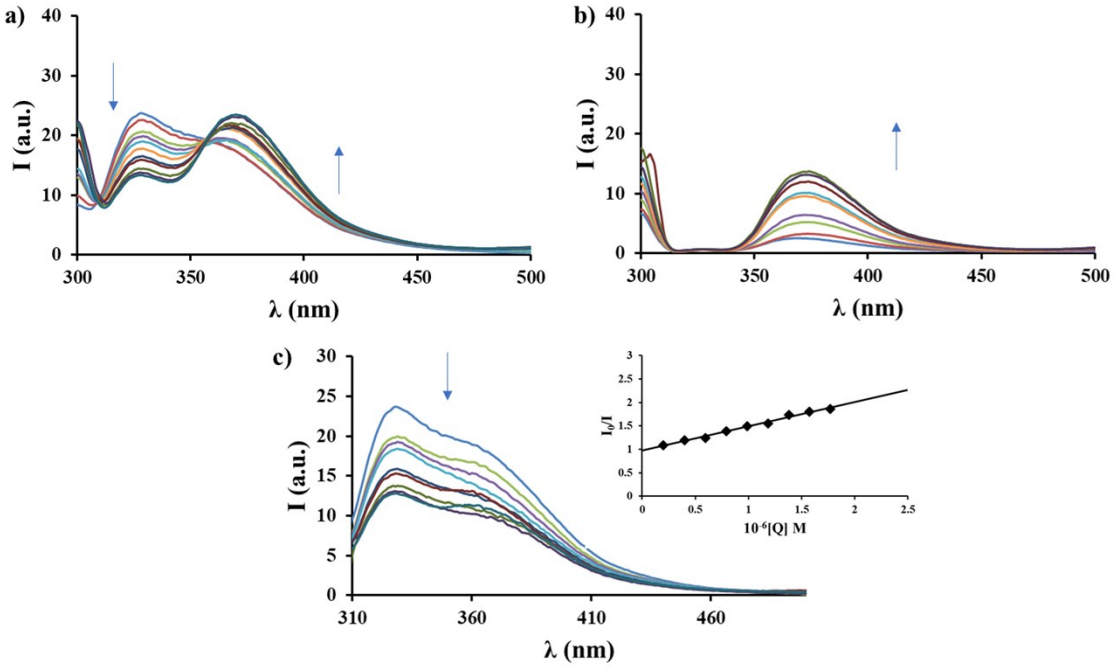

Fig. S2. a) Emission spectra of human serum albumin (2 μM; λex ,= 295 nm; λem = 365 nm) in the presence of the examined **Os2** complex, ratio complex : serum albumin was 1-10. b) Emission spectra of the examined **Os2** complex in the same concentrations as in spectra recorded with HSA c) Emission spectra of human serum albumin (2 μM; λex ,= 295 nm; λem = 365 nm) in the presence of the examined **Os2** complex, corrected for the emission spectra of the complex, ratio complex : serum albumin was 1-10. Insert graph: The dependence of I_0/I on the concentration [Q] (Q = complex). Arrows show changes in intensity after adding solutions of the growing concentration complex.

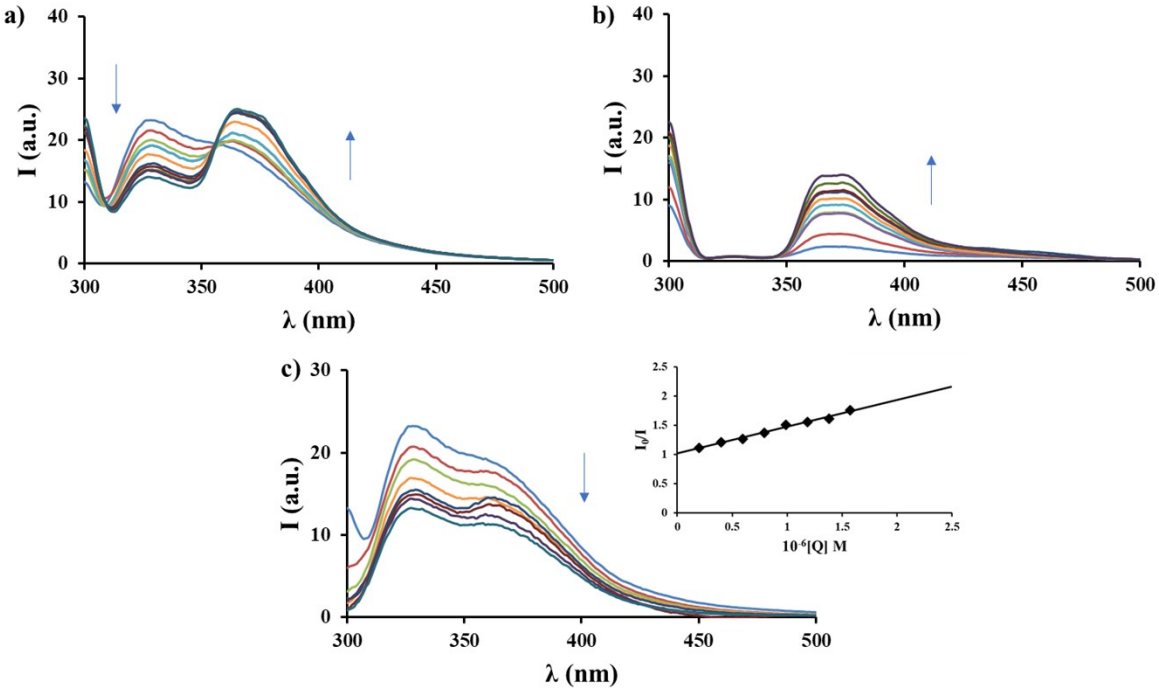

Fig. S3. a) Emission spectra of human serum albumin (2 μM; λex ,= 295 nm; λem = 365 nm) in the presence of the examined **Os3** complex, ratio complex : serum albumin was 1-10. b) Emission spectra of the examined **Os3** complex in the same concentrations as in spectra recorded with HSA c) Emission spectra of human serum albumin (2 μM; λex ,= 295 nm; λem = 365 nm) in the presence of the examined **Os3** complex, corrected for the emission spectra of the complex, ratio complex : serum albumin was 1-10. Insert graph: The dependence of I_0/I on the concentration [Q] (Q = complex). Arrows show changes in intensity after adding solutions of the growing concentration complex.

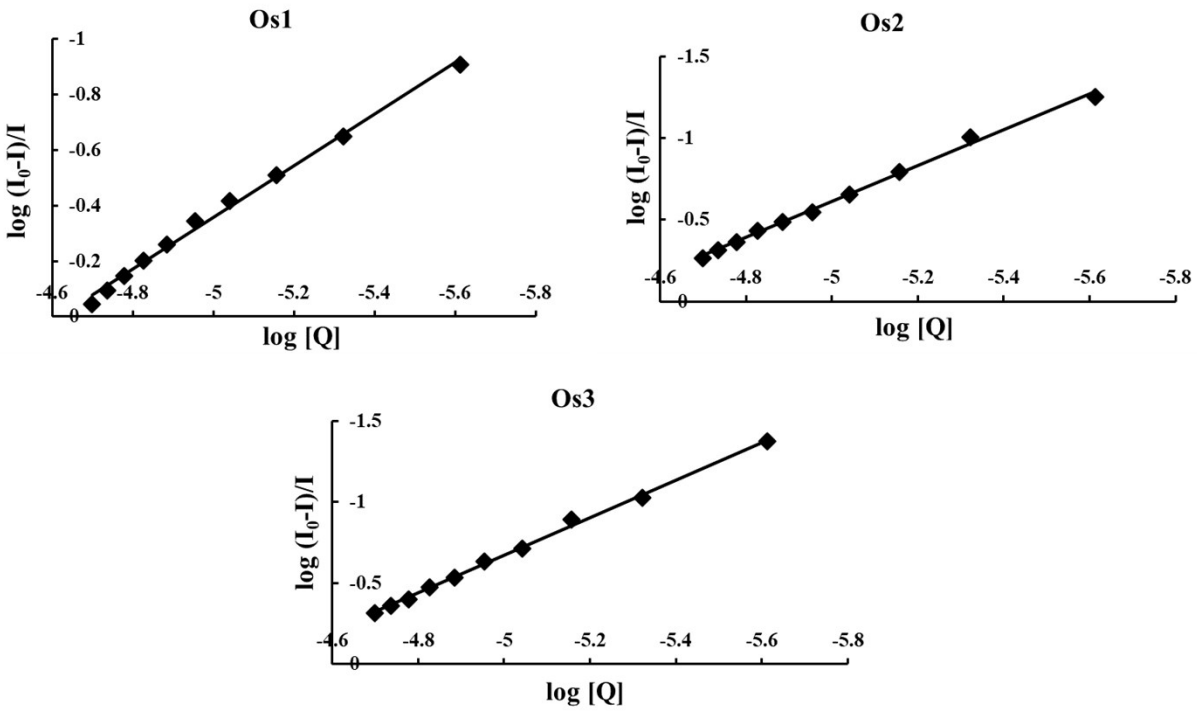

Fig. S4. Dependency log [(Io-I) / I] of log [Q] for the interaction between the examined **Os1-3** complexes and HSA; Q = (Complex **Os1-3**).

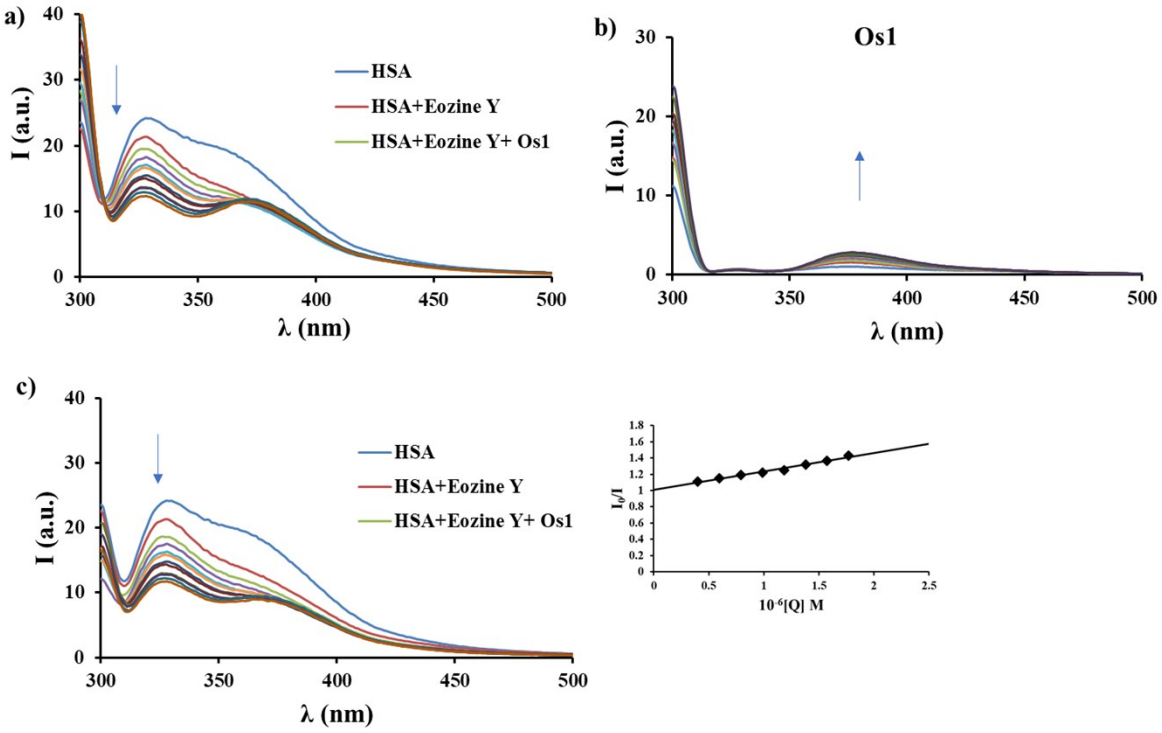

Fig. S5. a) Emission spectra of HSA (2 μM; λex ,= 295 nm; λem = 365 nm) in the presence of site marker Eosine Y and the examined **Os1** complex, ratio complex : serum albumin was 1-10. Site marker Eosin Y was added in the same concentration as HSA, ratio was 1:1. b) Emission spectra of the examined **Os1** complex in the same concentrations as in spectra recorded with HAS and Eosine Y c) Emission spectra of HSA (2 μM; λex ,= 295 nm; λem = 365 nm) in the presence of site marker Eosine Y the examined **Os1** complex, corrected for the emission spectra of the complex, ratio complex : serum albumin was 1-10. Site marker Eosin Y was added in the same concentration as HSA, ratio was 1:1. Insert graph: The dependence of I_0/I on the concentration [Q] (Q = complex). Arrows show changes in intensity after adding solutions of the growing concentration complex.

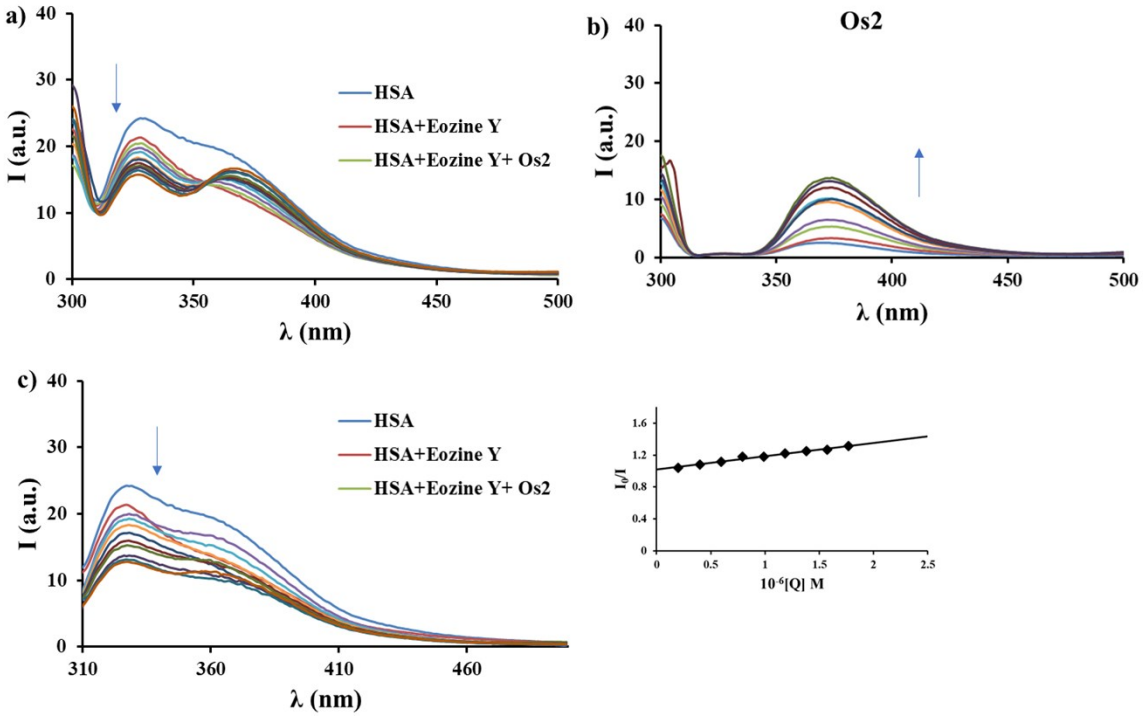

Fig. S6. a) Emission spectra of HSA (2 μM; λex ,= 295 nm; λem = 365 nm) in the presence of site marker Eosine Y and the examined **Os2** complex, ratio complex : serum albumin was 1-10. Site marker Eosin Y was added in the same concentration as HSA, ratio was 1:1. b) Emission spectra of the examined **Os2** complex in the same concentrations as in spectra recorded with HAS and Eosine Y c) Emission spectra of HSA (2 μM; λex ,= 295 nm; λem = 365 nm) in the presence of site marker Eosine Y the examined **Os2** complex, corrected for the emission spectra of the complex, ratio complex : serum albumin was 1-10. Site marker Eosin Y was added in the same concentration as HSA, ratio was 1:1. Insert graph: The dependence of I_0/I on the concentration [Q] (Q = complex). Arrows show changes in intensity after adding solutions of the growing concentration complex.

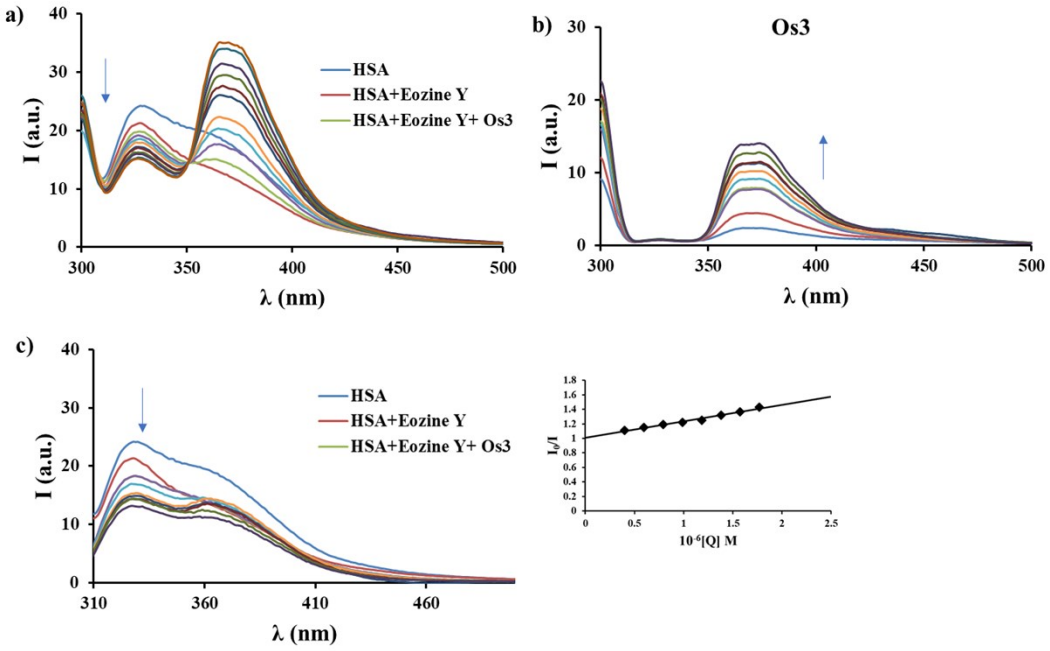

Fig. S7. a) Emission spectra of HSA (2 μM; λex ,= 295 nm; λem = 365 nm) in the presence of site marker Eosine Y and the examined **Os3** complex, ratio complex : serum albumin was 1-10. Site marker Eosin Y was added in the same concentration as HSA, ratio was 1:1. b) Emission spectra of the examined **Os3** complex in the same concentrations as in spectra recorded with HAS and Eosine Y c) Emission spectra of HSA (2 μM; λex ,= 295 nm; λem = 365 nm) in the presence of site marker Eosine Y the examined **Os3** complex, corrected for the emission spectra of the complex, ratio complex : serum albumin was 1-10. Site marker Eosin Y was added in the same concentration as HSA, ratio was 1:1. Insert graph: The dependence of I_0/I on the concentration [Q] (Q = complex). Arrows show changes in intensity after adding solutions of the growing concentration complex.

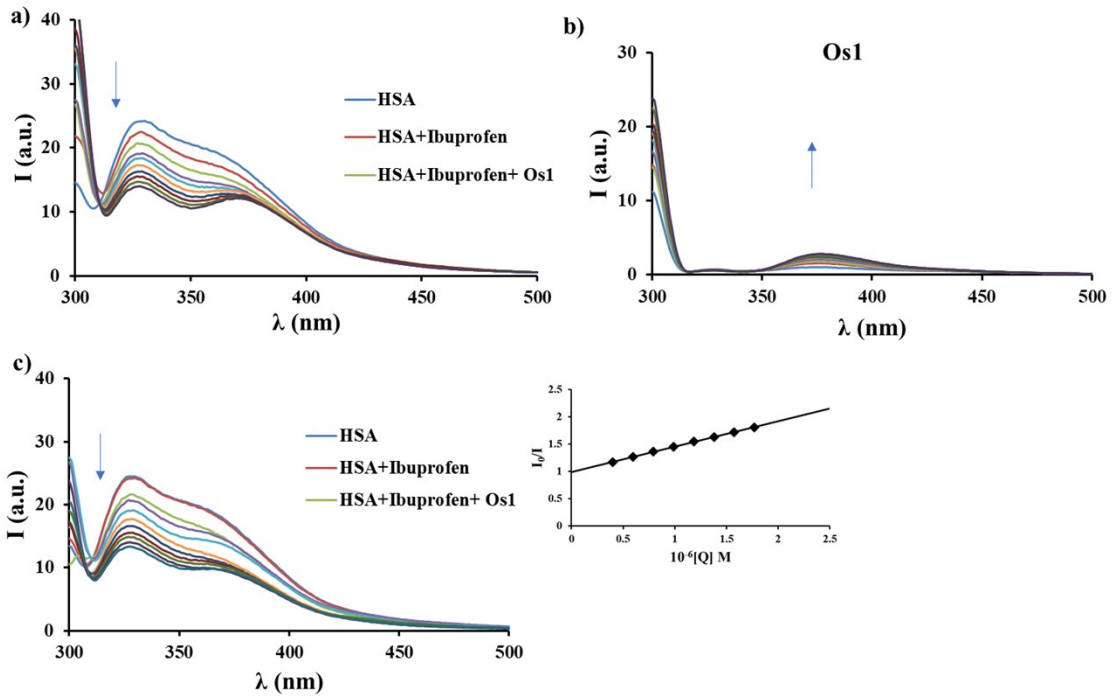

Fig. S8. a) Emission spectra of HSA (2 μM; λex ,= 295 nm; λem = 365 nm) in the presence of site marker Ibuprofen and the examined **Os1** complex, ratio complex : human serum albumin was 1-10. Site marker Ibuprofen was added in the same concentration as HSA, ratio was 1:1. b) Emission spectra of the examined **Os1** complex in the same concentrations as in spectra recorded with HAS and Ibuprofen c) Emission spectra of HSA (2 μM; λex ,= 295 nm; λem = 365 nm) in the presence of site marker Ibuprofen the examined **Os1** complex, corrected for the emission spectra of the complex, ratio complex : serum albumin was 1-10. Site marker Ibuprofen was added in the same concentration as HSA, ratio was 1:1. Insert graph: The dependence of I_0/I on the concentration [Q] (Q = complex). Arrows show changes in intensity after adding solutions of the growing concentration complex.

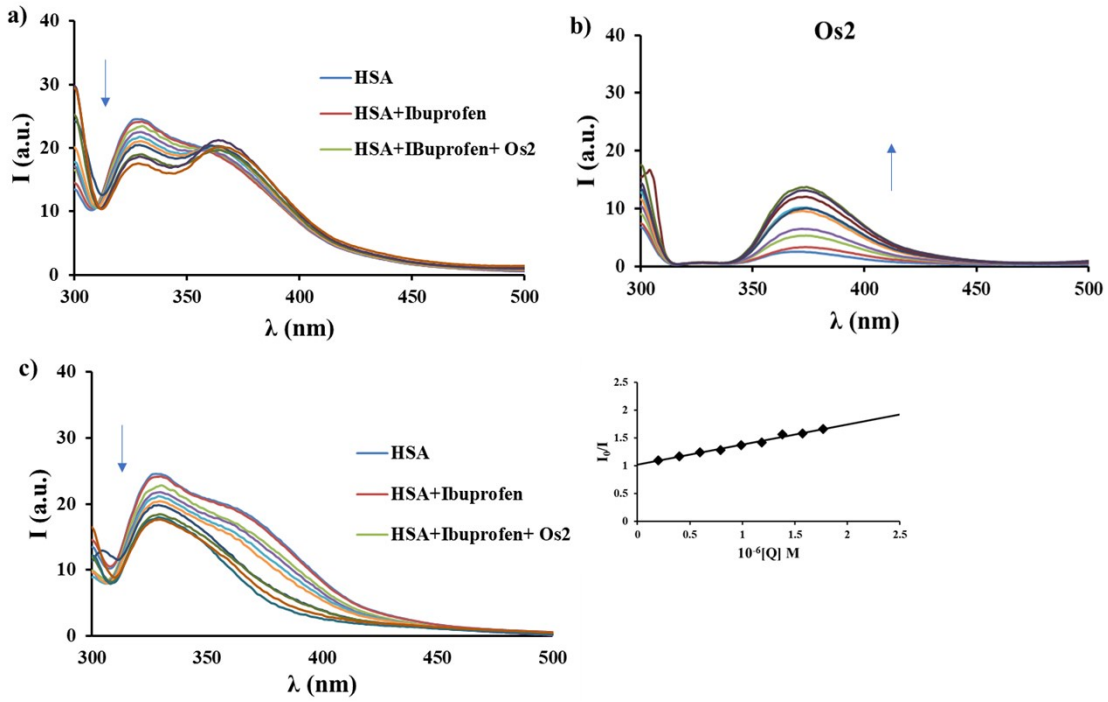

Fig. S9. a) Emission spectra of HSA (2 μM; λex ,= 295 nm; λem = 365 nm) in the presence of site marker Ibuprofen and the examined **Os2** complex, ratio complex : human serum albumin was 1-10. Site marker Ibuprofen was added in the same concentration as HSA, ratio was 1:1. b) Emission spectra of the examined **Os2** complex in the same concentrations as in spectra recorded with HAS and Ibuprofen c) Emission spectra of HSA (2 μM; λex ,= 295 nm; λem = 365 nm) in the presence of site marker Ibuprofen the examined **Os2** complex, corrected for the emission spectra of the complex, ratio complex : serum albumin was 1-10. Site marker Ibuprofen was added in the same concentration as HSA, ratio was 1:1. Insert graph: The dependence of I_0/I on the concentration [Q] (Q = complex). Arrows show changes in intensity after adding solutions of the growing concentration complex.

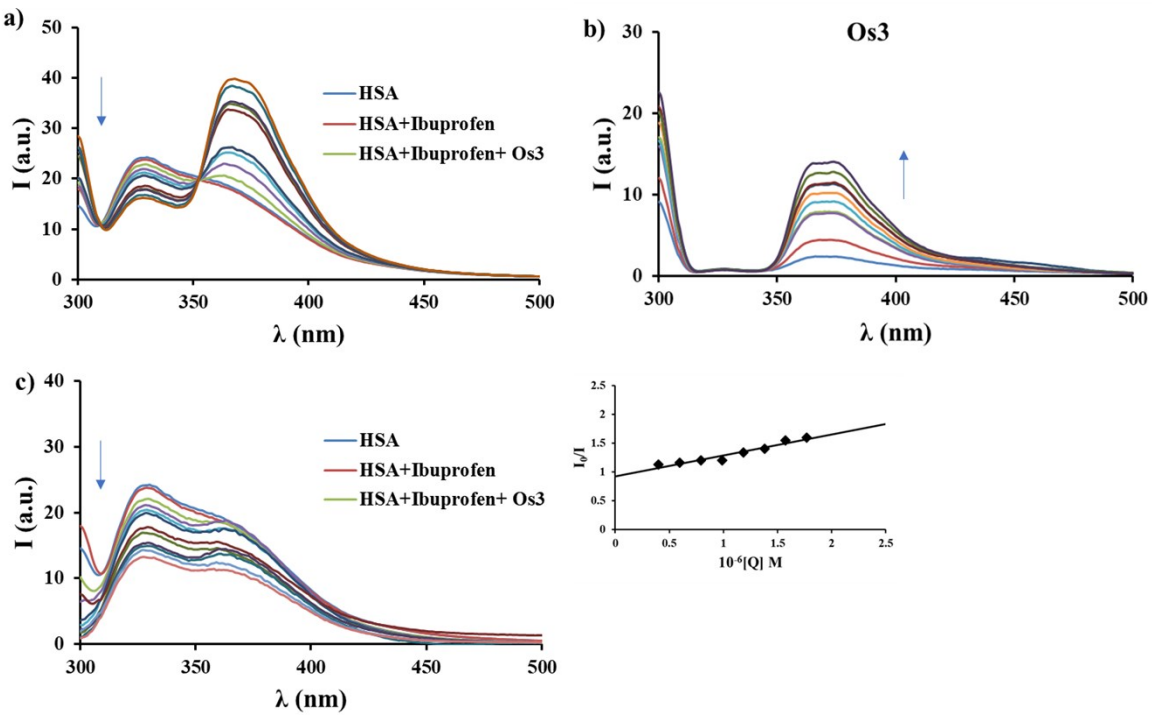

Fig. S10. a) Emission spectra of HSA (2 μM; λex ,= 295 nm; λem = 365 nm) in the presence of site marker Ibuprofen and the examined **Os3** complex, ratio complex : human serum albumin was 1-10. Site marker Ibuprofen was added in the same concentration as HSA, ratio was 1:1. b) Emission spectra of the examined **Os3** complex in the same concentrations as in spectra recorded with HAS and Ibuprofen c) Emission spectra of HSA (2 μM; λex ,= 295 nm; λem = 365 nm) in the presence of site marker Ibuprofen the examined **Os3** complex, corrected for the emission spectra of the complex, ratio complex : serum albumin was 1-10. Site marker Ibuprofen was added in the same concentration as HSA, ratio was 1:1. Insert graph: The dependence of I_0/I on the concentration [Q] (Q = complex). Arrows show changes in intensity after adding solutions of the growing concentration complex.

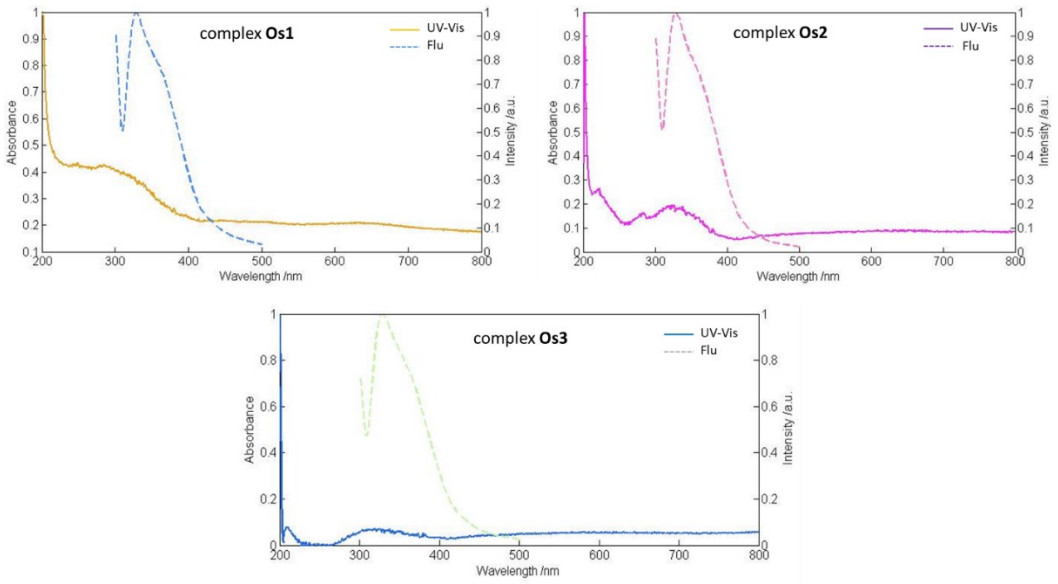

Fig. S11. The overlap of the absorption spectrum of a complexes **Os1-3** and fluorescence spectrum of HSA. The ration of **Os1-3** complexes and HAS is 1:1.

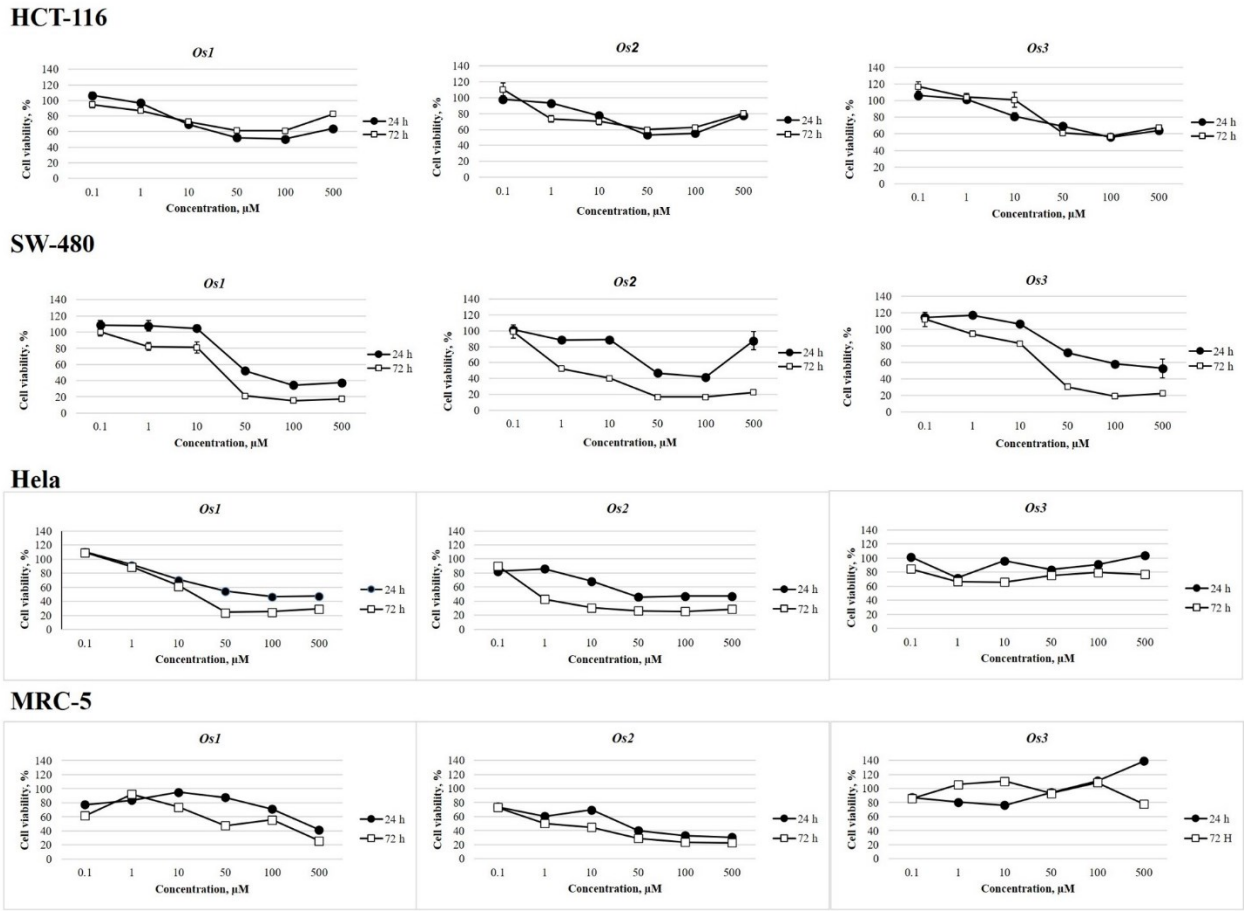

Fig. S12. Cell viability after 24h and 72h of exposure, expressed in percentages of viable cells.

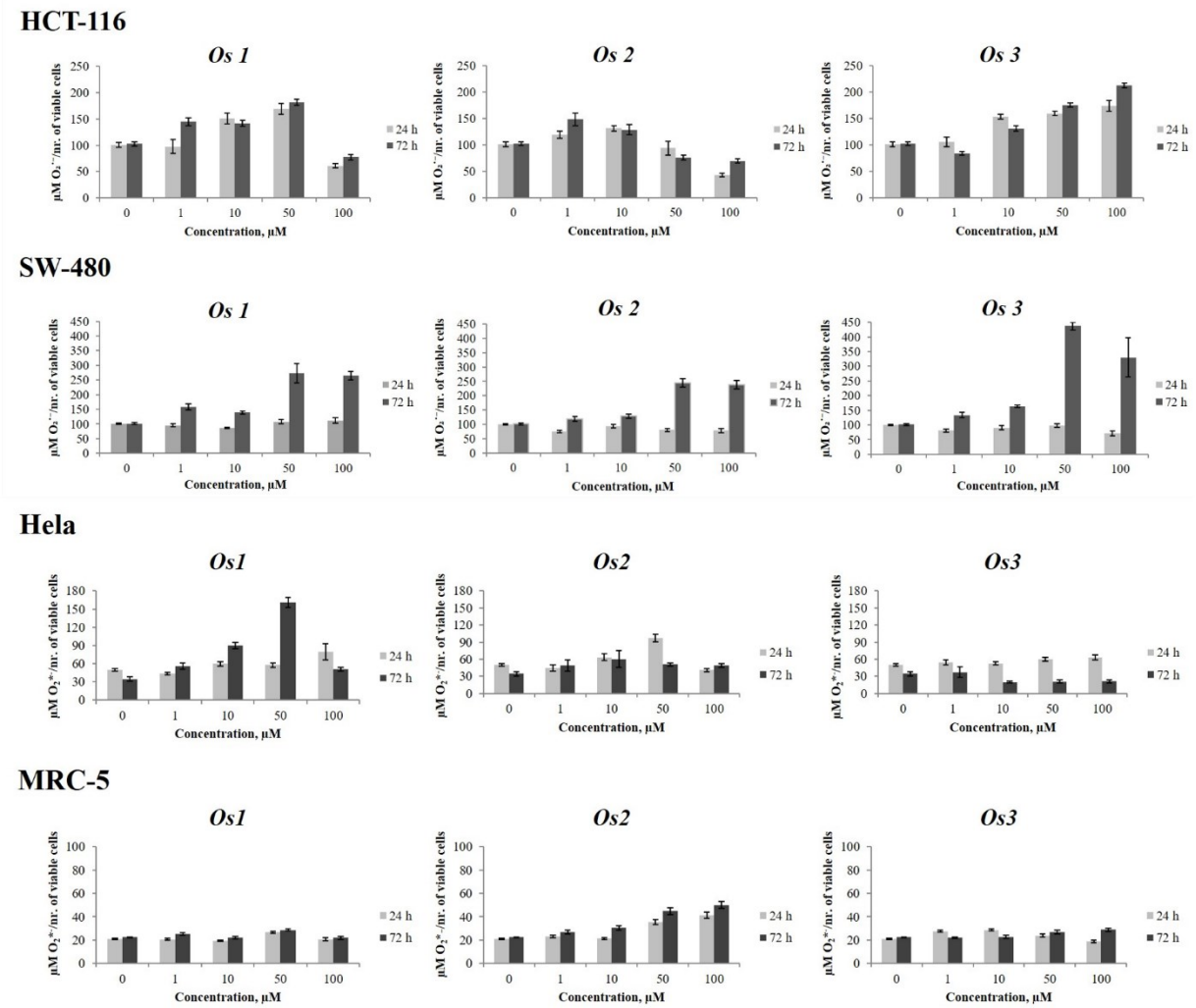

Fig. S13. E□ects of **Os1-3** complexes on HCT-116, SW-480, Hela and MRC-5 cell lines, expressed as the $O_2^{\bullet-}$ concentration after 24h and 72h of exposure.

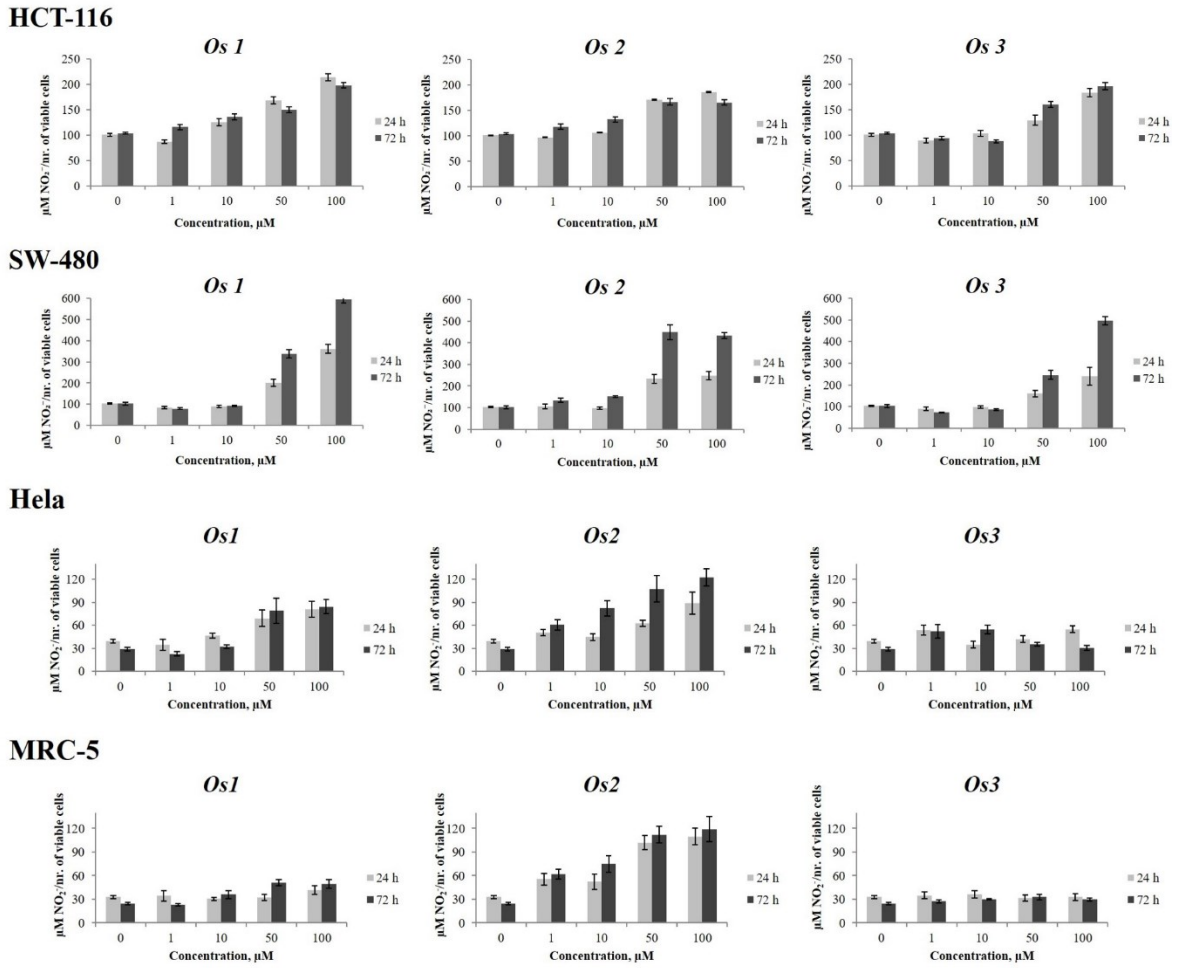

Fig. S14. E□ects of **Os1-3** complexes on HCT-116, SW-480, Hela and MRC-5 cell lines, expressed as the NO_2^- concentration after 24h and 72h of exposure.

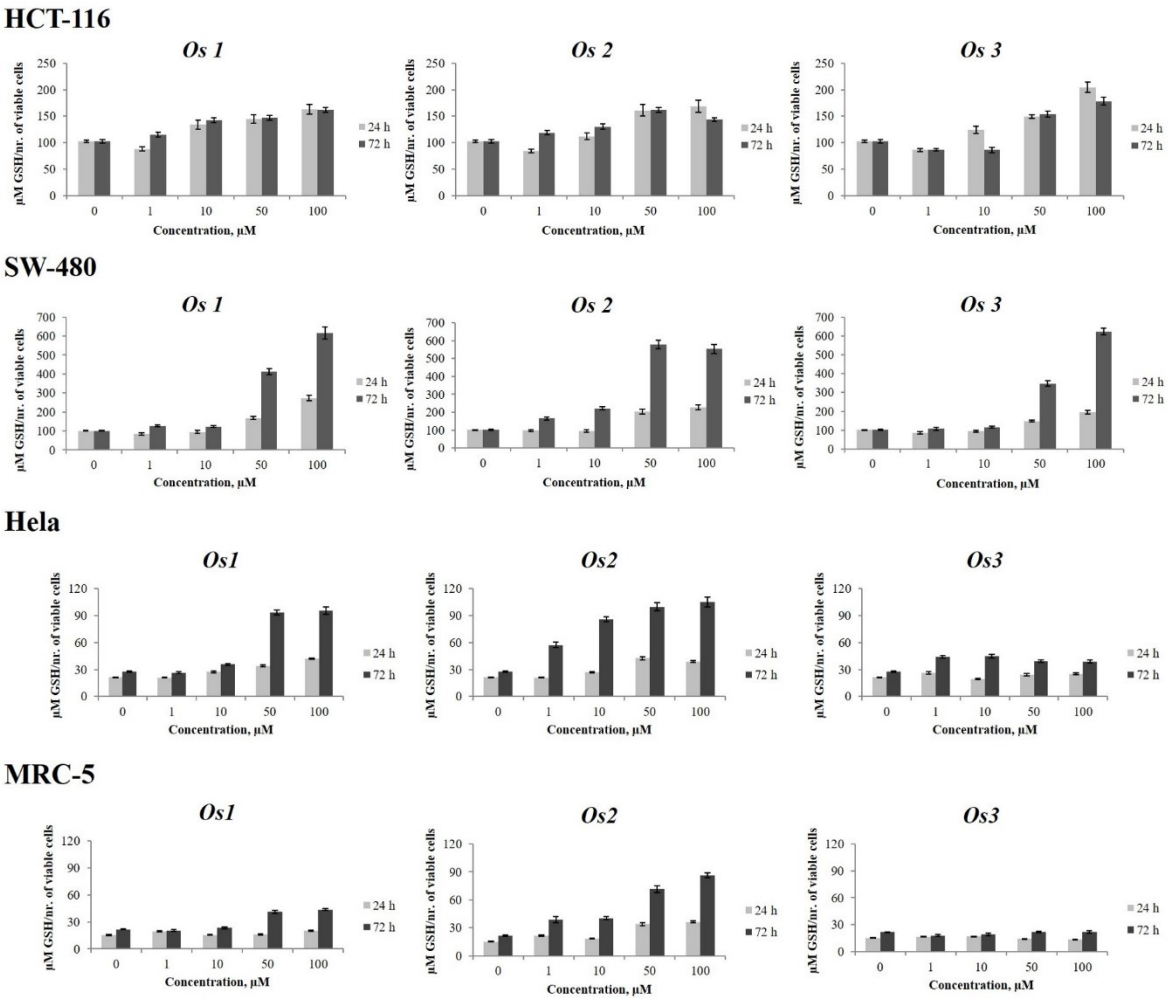

Fig. S15. E□ects of **Os1-3** complexes on HCT-116, SW-480, Hela and MRC-5 cell lines, expressed as the GSH concentration after 24h and 72h of exposure.

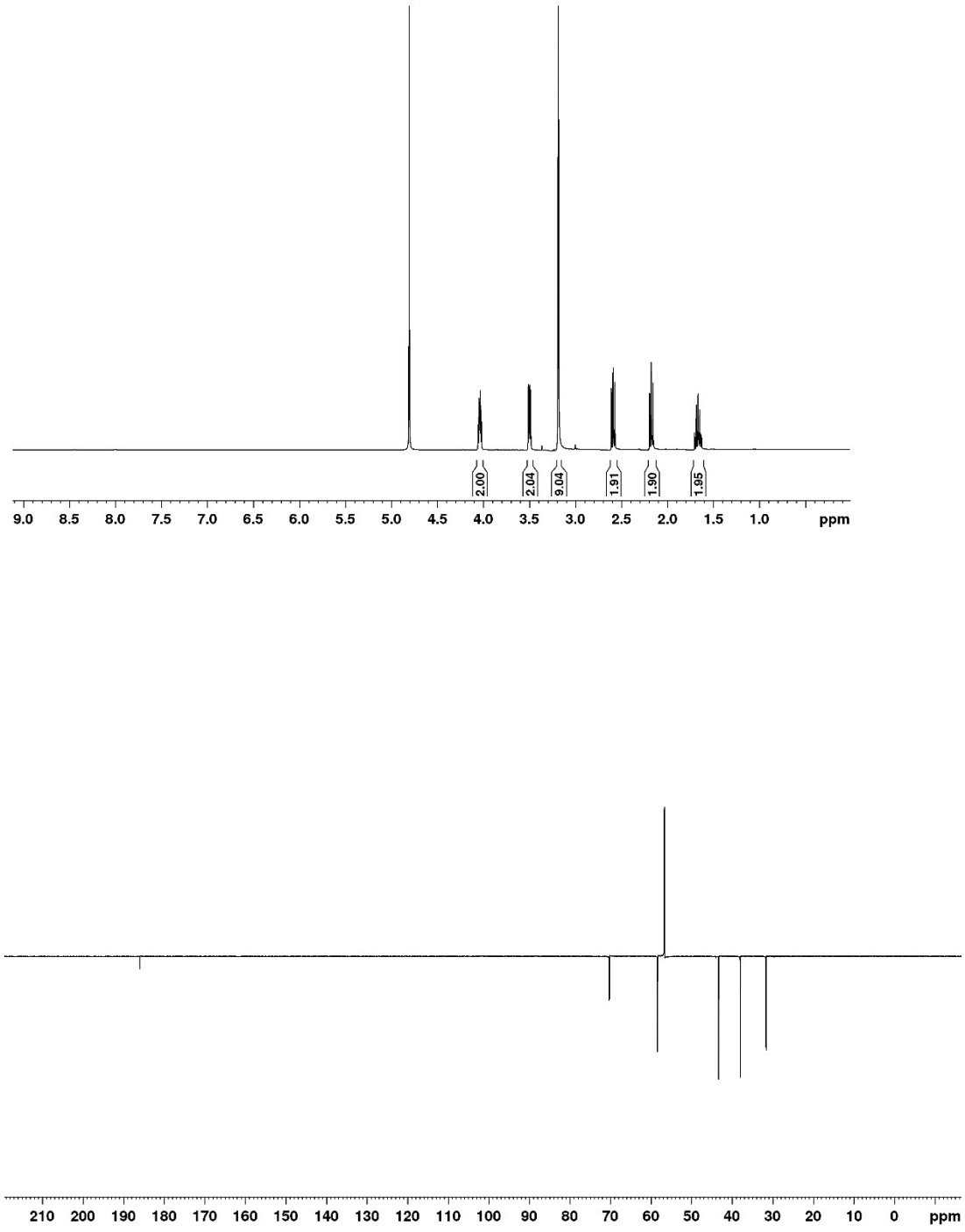

Fig. S16. ^{1}H NMR and ^{13}C NMR spectra of IL4

^{1}H (D_2O): 1.67 (*m*, 2H, C***H*****$_2$**CH_2COO^-**)**, 2.17 (*t*, 2H, C***H*****$_2$**COO^-**)**, 2.60 (t, 2H, C***H*****$_2$**NH_2), 3.19 (bs, 9H, N(C***H*****$_3$**$)_3$), 3.50 (*m*, 2H, C***H*****$_2$**$N(CH_3)_3$), 4.04 (*m*, 2H, C***H*****$_2$**OH).

^{13}C (D_2O): 31.64 (***C***$H_2CH_2COO^-$), 38.00 (***C***H_2COO^-), 43.34 (***C***H_2NH_2), 56.67, 56.71, 56.75 ($N(***C***H_3)_{3,}$), 58.42 ($HO***C***H_2CH_2N(CH_3)_3$), 70.27, 70.30, 70.33 (***C***$H_2N(CH_3)_3$), 185.97 (**C**=O).

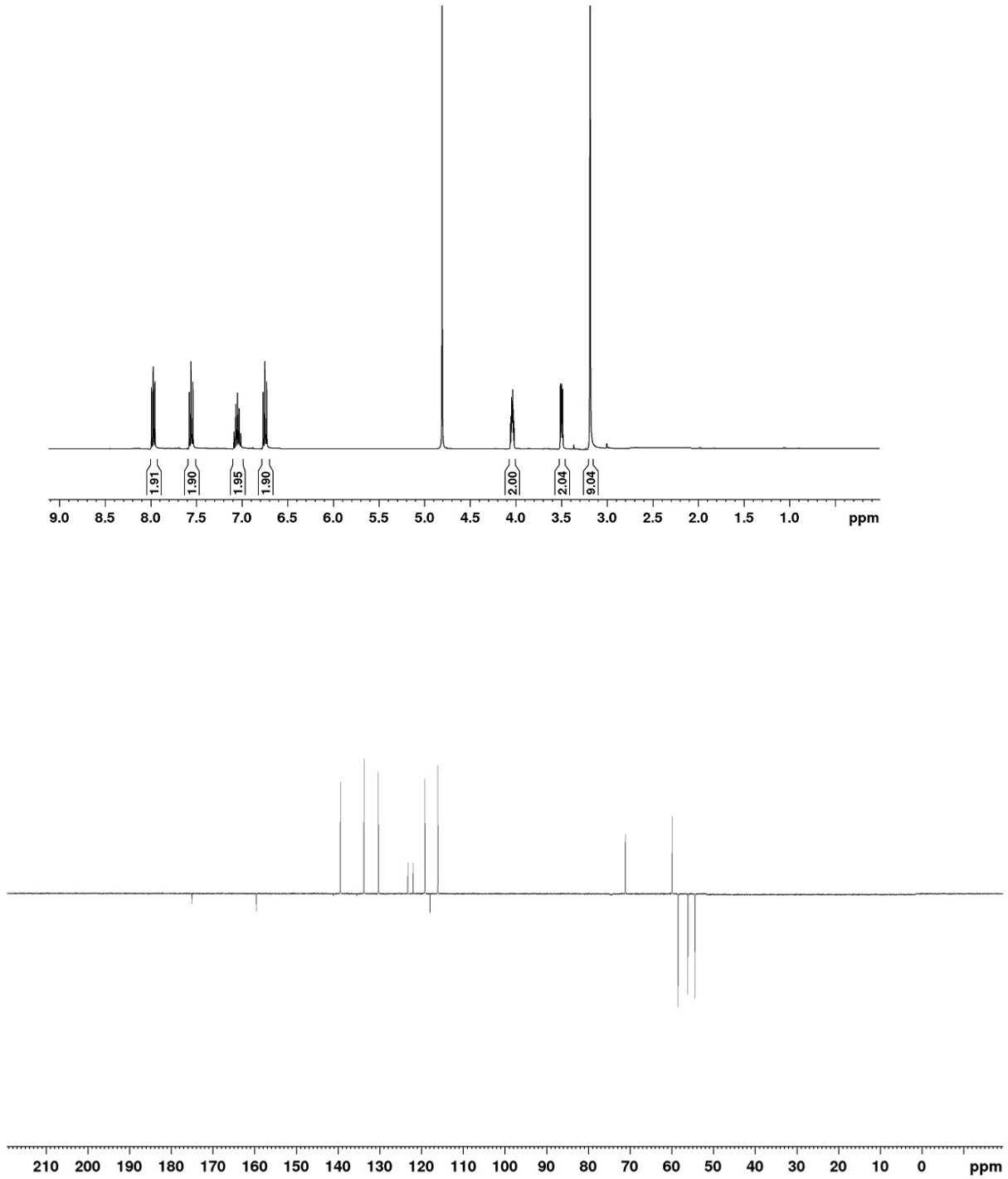

Fig. S17. ^{1}H NMR and ^{13}C NMR spectra of IL5

^{1}H NMR (D_2O): 3.12 (bs, 9H, $N(C\boldsymbol{H}_3)_3$), 3.52 (*m*, 2H, $C\boldsymbol{H}_2N(CH_3)_3$), 4.07 (*m*, 2H, $C\boldsymbol{H}_2OH$), 7.31, 7.38 and 7.41 (2xs, 5H, H-6, H-7, H-8, H-9, H-10); 7.61 and 7.67 (2*xs*. 2H. H-4 and H-5)

^{13}C NMR (D_2O): 55.21, 56.09, 56.34 (N(***C***$H_3)_3$,), 59.26 (HO***C***$H_2CH_2N(CH_3)_3$), 70.35 (***C***$H_2N(CH_3)_3$), 124.34 i 125.65 (C-4 i C-5); 129.65 (C-6); 130.21 (C-7), 130.86 (C-8), 135.11 (*d*. C-2), 141.73 (C-9) and 174.05 (*C*OO^-)

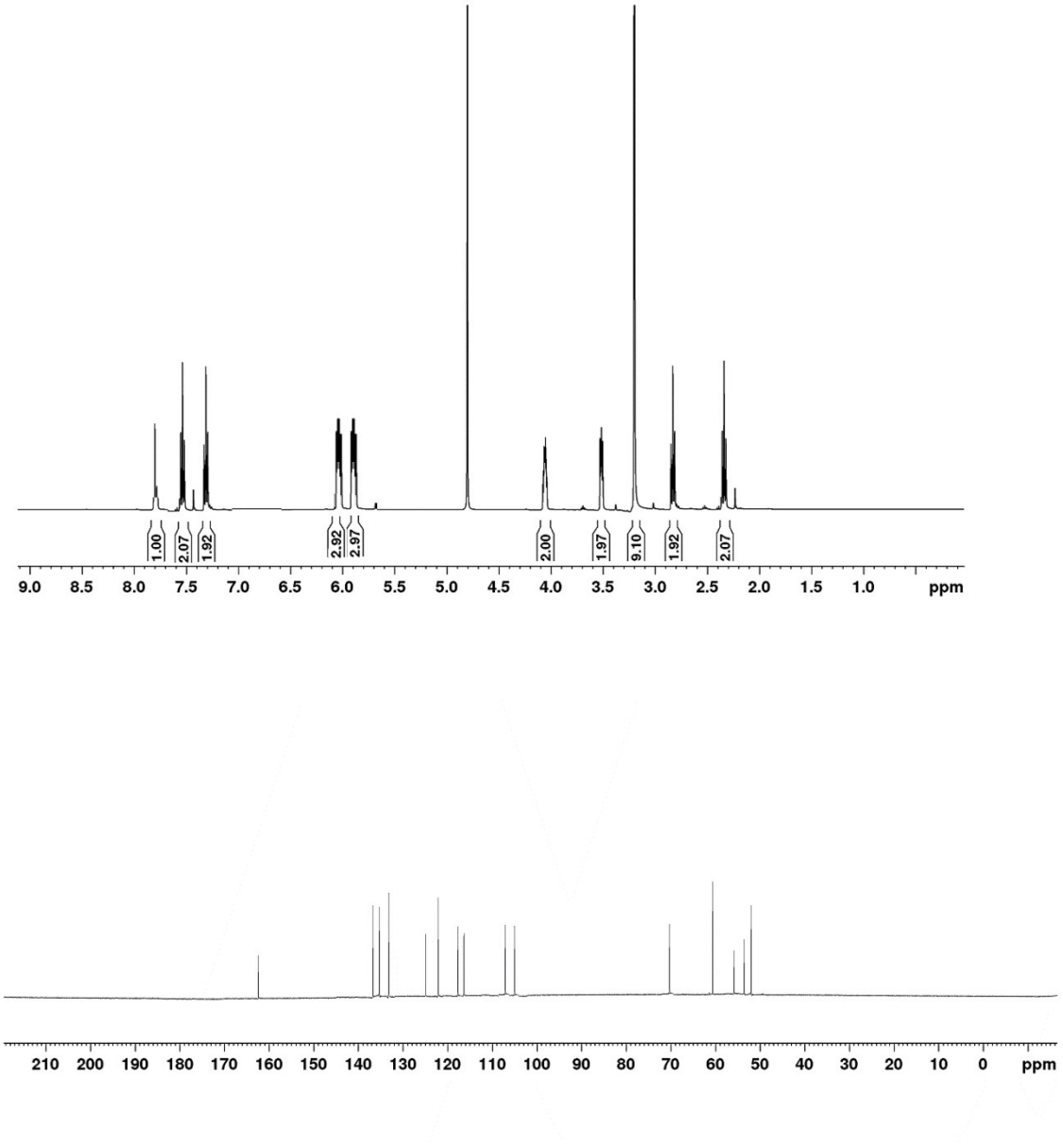

Fig. S18. ^{1}H NMR and ^{13}C NMR spectra of IL7

^{1}H NMR (D_2O):): 3.12 (bs, 9H, N(C*H*$_3$)$_3$), 3.71 (*m*, 2H, C*H*$_2$N(CH$_3$)$_3$), 4.19 (*m*, 2H, C*H*$_2$OH), 5.81 and 6.04 (*bs* 6H, O-C*H*$_3$), 7.41 and 7.53 (2*xs*, 2H, H-1' i H-2'), 7.74 (*dd*, 1H, C-O*H*)

^{13}C NMR (D_2O): 55.33, 55.49, 55.84 (N(*C*H$_3$)$_3$), 59.26 (HO*C*H$_2$CH$_2$N(CH$_3$)$_3$), 71.04 (*C*H$_2$N(CH$_3$)$_3$), 106.23 and 106.33 (O-*C*H$_3$), 118.09 (C-3′), 119.22 (C-1′), 122.23 (C-5′), 135.33 (C-6′), 137.36 (C-4′), 139.41 (C-2'), 165.44 (C-7′).

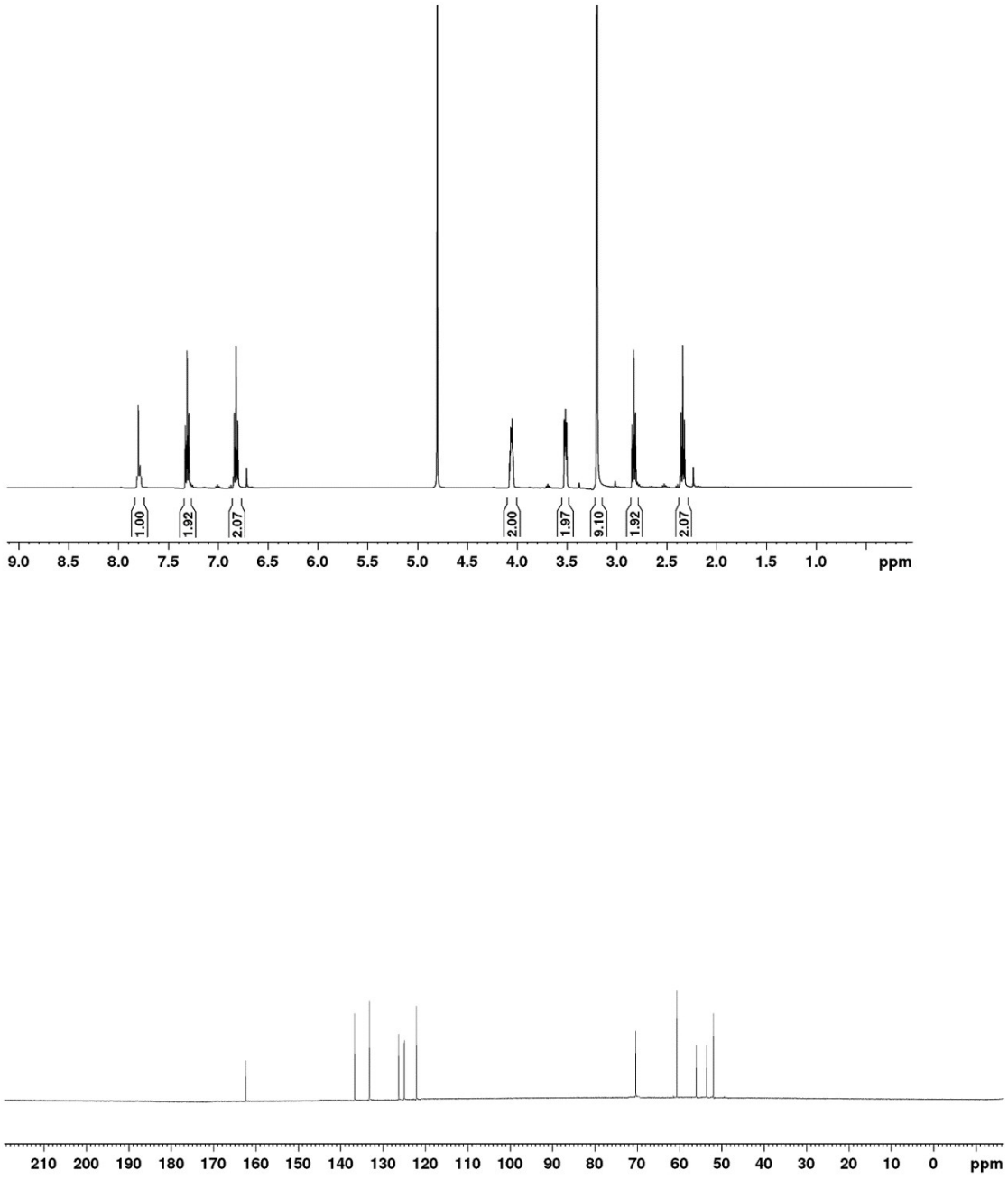

Fig. S19. ^{1}H NMR and ^{13}C NMR spectra of IL8

^{1}H NMR (D_2O):): 3.08 (bs, 9H, $N(CH_3)_3$), 3.65 (*m*, 2H, $CH_2N(CH_3)_3$), 4.12 (*m*, 2H, CH_2OH), 6.83 (*d*, 1H, $J_{3',4'}$= 8.2 Hz, H-1'), 6.89 (t, 1H, *J*= 7.5 Hz, H-5'), 7.27 and 7.36 (2*xs*, 2H, H-2' i H-4'), 7.74 (*dd*, 1H, $J_{4',6'}$= 1.3 Hz, $J_{5',6'}$= 7.8 Hz H-3′).

^{13}C NMR (D_2O): 54.93, 55.29, 55.74 ($N(CH_3)_3$), 58.83 ($HOCH_2CH_2N(CH_3)_3$), 70.02 ($CH_2N(CH_3)_3$), 121.09 (C-3′), 123.22 (C-1′), 124.23 (C-5′), 130.33 (C-6′), 133.79 (C-4′), 135.41 (C-2'), 162.21 (C-7′).

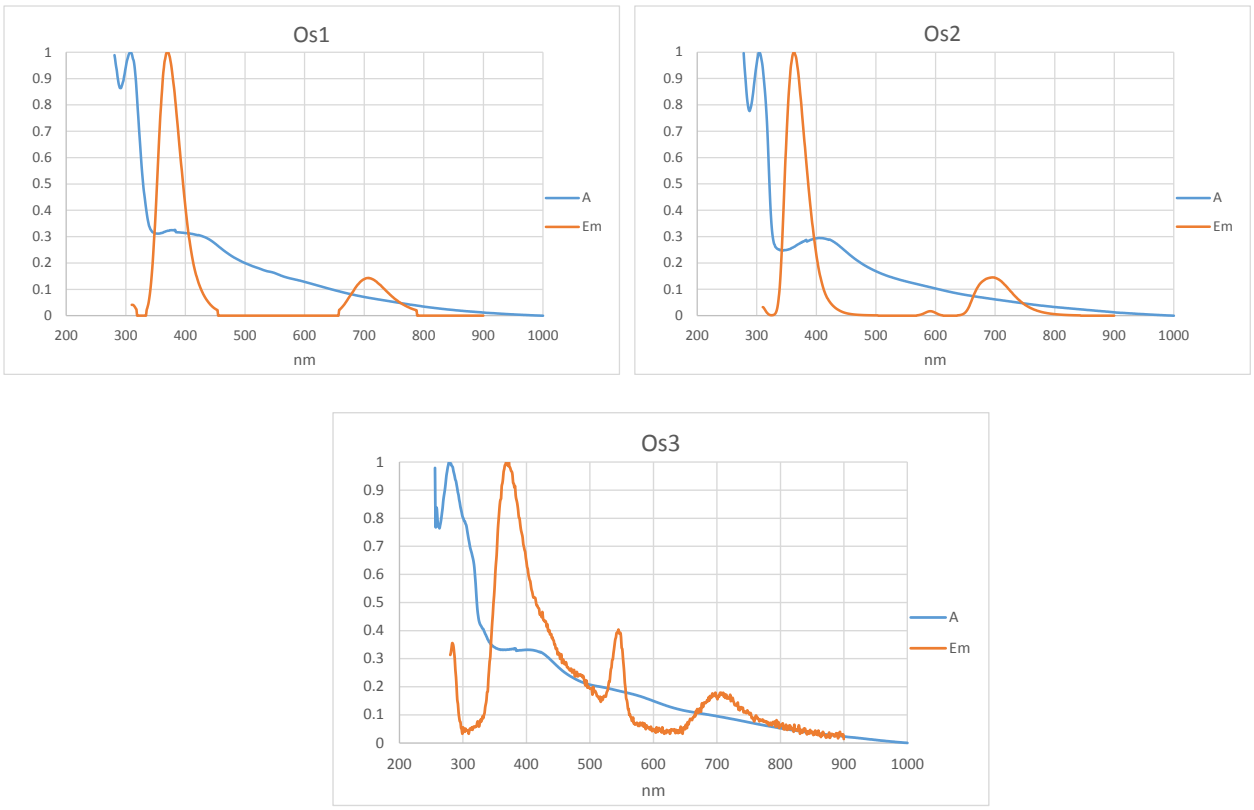

Fig. S20. Absorption and emission spectra of **Os1-3** complexes in water/dmf solution.